Scientific Research Publishing

Journal of Minerals and Materials Characterization and Engineering, 2025, 13(6), 381-395
https://www.scirp.org/journal/jmmce
ISSN Online: 2327-4085
ISSN Print: 2327-4077

Petrographic and Geochemical Characteristics of the Séguéla Granitoids, Northwestern Côte d'Ivoire

Brice Roland Kouassi[1*], Brou Koffi Joseph[2], Kouadio David Koffi[2], Aissata Ouedraogo[2], Alain Nicaise Kouamelan[2]

[1]Département de Géosciences, UFR Sciences Biologiques, Université Peleforo Gon Coulibaly, Korhogo, Côte d'Ivoire
[2]Laboratoire de Géologie, Ressources Minérales et Energétiques, UFR Sciences de la Terre et des Ressources Minières, Université Félix Houphouët-Boigny (UFHB, Abidjan-Cocody), Abidjan, Côte d'Ivoire
Email: *broland.kouassi@gmail.com

How to cite this paper: Kouassi, B.R., Joseph, B.K., Koffi, K.D., Ouedraogo, A. and Kouamelan, A.N. (2025) Petrographic and Geochemical Characteristics of the Séguéla Granitoids, Northwestern Côte d'Ivoire. *Journal of Minerals and Materials Characterization and Engineering*, **13**, 381-395.
https://doi.org/10.4236/jmmce.2025.136021

Received: October 11, 2025
Accepted: November 17, 2025
Published: November 20, 2025

Abstract

This paper focuses on the study of granitoids within the large transition zone of the seguela region in northwestern cote d'ivoire. This area is characterized, in its northern part, by the presence of a large porphyroid granitoid massif. Petrographic and geochemical analyses allow us to group the lithological units of the study area into three main facies: 1) granites, 2) granodiorite, and 3) migmatites. The granites have a calc-alkaline affinity and a slightly peraluminous chemistry, whereas the granodiorite and migmatites are generally metaluminous. The migmatites are moderately to strongly calc-alkaline. Similarities in the multi-element and rare-earth element spectra of the different lithologies suggest a common source of emplacement. However, the positive eu anomalies in the granites and the negative anomalies in the granodiorite and migmatites may indicate that the granites derived from the partial melting of a more or less differentiated crustal protolith with plagioclase remaining in the residue. We can therefore consider that the studied granitoids and migmatites were generated in subduction zones. This subduction is consequently responsible for the release of potassium-rich fluids, leading to the formation of pink granites rich in potassium feldspar.

Keywords

Granitoids, Migmatites, Calc-Alkaline, Séguéla, Partial Melting

1. Introduction

The Séguéla region, which constitutes the study area, is located in the northwestern part of Côte d'Ivoire, West Africa. Côte d'Ivoire, which lies within the West African Craton, is geologically dominated by two major domains: the Archean and the Paleoproterozoic. The study area belongs to the Archean-Proterozoic transition zone, situated to the east of the Archean Domain and the Sassandra Fault, and along the western margin of the Paleoproterozoic Domain (**Figure 1**). The various lithologies observed in the area include tonalitic gneisses, migmatites, volcano-plutonic belts, granitoid plutons of diverse composition, and metasedimentary rocks intruded by plutons [1]. Previous works [2]-[5] have shown that this western part of the Archean domain in Côte d'Ivoire is composed of gray tonalitic and trondhjemitic gneisses, charnockites, greenstone rocks metamorphosed under granulite facies, magnetite-bearing banded quartzites, and biotite migmatites. These formations are intruded by pink granites and basic-ultrabasic complexes. This entire assemblage has been attributed to the Leonian (3.5 - 2.9 Ga) and Liberian (2.9 - 2.6 Ga) orogenic cycles by earlier authors [6].

In Côte d'Ivoire, the crustal evolution experienced three major Precambrian orogenies: the Liberian, Leonian, and Eburnean. The resulting basement, older than 1.6 Ga, occupies almost the entire territory except for the extreme south, which is covered by the coastal basin [7]. The granitoids make up the majority of the outcrops of this Precambrian basement and are highly diverse, thus representing significant geological components of the country [8]. The granitoids of Côte d'Ivoire have been the subject of numerous lithostratigraphic and geochemical studies aimed at understanding their genesis [9]-[14]. Following in the footsteps of these earlier works, we have focused particular attention on the granitoids of the Séguéla region, which is known as a diamond-bearing zone. It is therefore necessary to undertake petrographic and geochemical studies to contribute to a better understanding of these rocks in this region.

2. Geological Setting

Geologically, Côte d'Ivoire forms part of the West African Craton, more specifically within the Man-Leo Shield [6]. The country is predominantly underlain by a Precambrian basement (97.5%) and a younger sedimentary cover (2.5%). This basement, which includes the study area, is subdivided into two major domains: the Kenema-Man Domain to the west and the Baoulé-Mossi Domain to the east, separated by the major transcurrent Sassandra Fault. Previous studies [2] [4] [15]-[17] have shown that the Kenema-Man Domain is largely composed of Archean terrains made up of a granito-gneissic basement complex and supracrustal greenstone belts. These rocks were successively affected by the Leonian orogeny (3.4 - 3.0 Ga) [18] [19] and the Liberian orogeny (2.9 - 2.7 Ga) [2] [18], and were later overprinted by the Eburnean orogeny [20]-[22]. In contrast, the Baoulé-Mossi Domain to the east is mainly composed of Paleoproterozoic formations deformed and metamorphosed during the Eburnean event [20]-[23]. The lithologies of the Kenema-Man Domain are predominantly TTG-type (tonalite-trondhjemite-granodiorite) suites, associated with kinzigitic metasediments, magnetite-bearing quartzites, and granulitic metabasalts [2] [4] [15] [21] [24]. Between the Archean and Paleoproterozoic domains sensu stricto lies a transition zone, bounded by the Sassandra Fault to the west and approximately longitude 6˚W to the east. This zone exhibits clear Archean inheritance, marked by crustal relics dated at about 3.2 Ga in the southern part of the SASCA Domain [4] [25] [26].

Located in the west-central part of Côte d'Ivoire, the Séguéla region belongs to this Archean-Proterozoic transition zone, lying east of the Archean Domain and the Sassandra Fault, and along the western margin of the Paleoproterozoic Domain (**Figure 1(A)**). The region is well known for its diamondiferous field, fed by kimberlite and lamproite dykes (**Figure 1(A)**). These dykes intrude granite plutons separated by amphibolite panels belonging to the Birimian formations. The granites are monzonitic, containing biotite and hornblende, and display well-differentiated pegmatitic and aplitic cupolas, as well as porphyroid margins [1] (**Figure 1(B)**). Their N170˚ orientation is structurally controlled by the contact between the Archean and Paleoproterozoic lithospheres of the West African Craton.

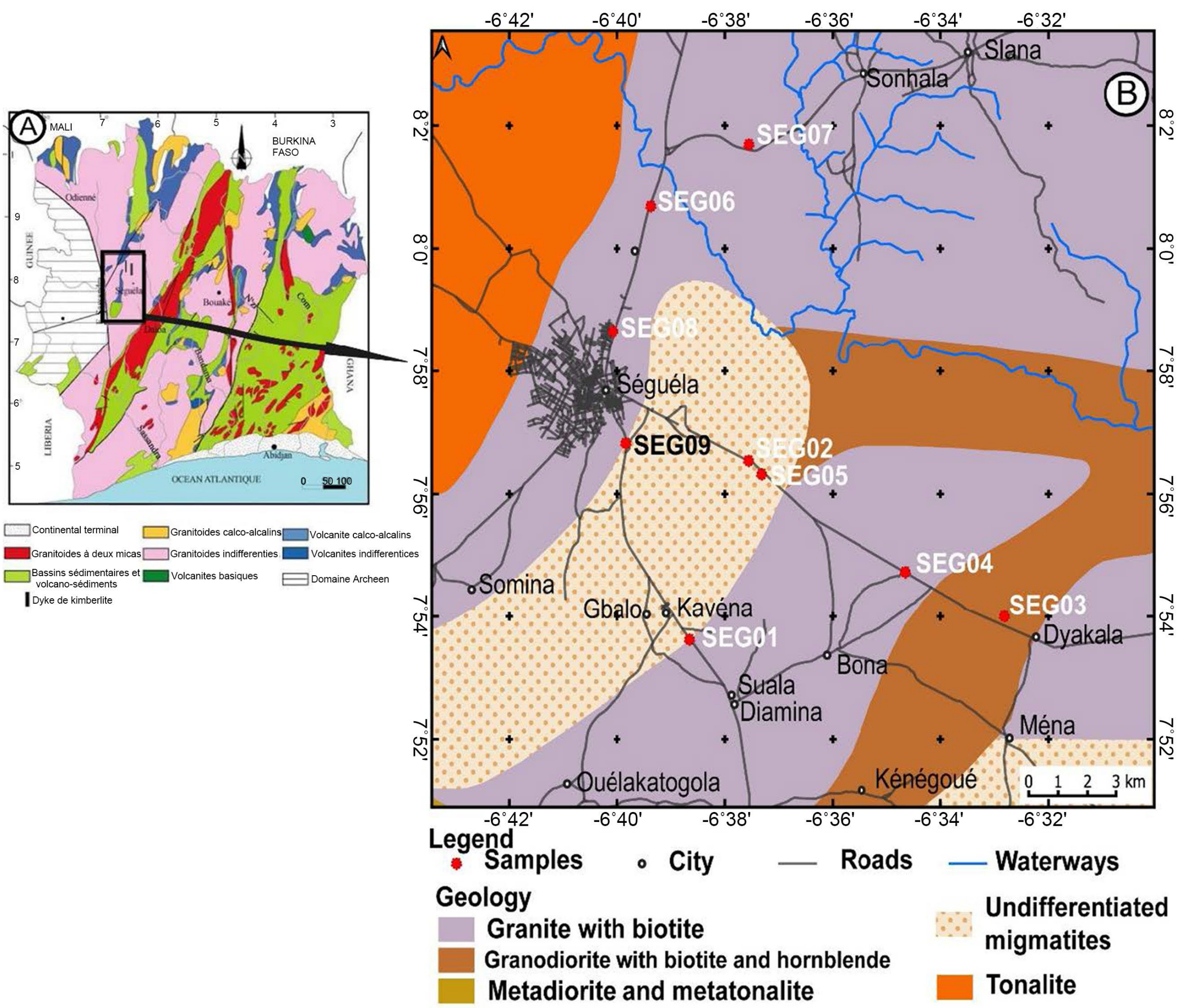

Figure 1. Geological map of Côte d'Ivoire and the study area. A-Simplified geological map of Côte d'Ivoire (modified after [27]). B-Geological map of the Séguéla region (published by the Directorate of Mines and Geology) showing the sampling locations.

3. Analytical Method

3.1. Sample Collection and Optical Petrography

The studied samples belong to the granitoids of the Séguéla region (**Figure 1(B)**). In the field, the various lithologies were first described macroscopically before sampling for more detailed analyses, including microscopic observations and whole-rock geochemical analyses. Accordingly, nine (09) thin sections were prepared from fresh samples for petrographic examination under a polarizing microscope at the Laboratory of Geology and Mineral Resources, Department of Earth and Mineral Resources Sciences, Félix Houphouët-Boigny University, Cocody.

3.2. Bulk Whole-Rock Analysis

The aim of the geochemical study is to investigate the geochemical characteristics of the rocks in order to understand the distribution of chemical elements within these different lithologies, as well as the factors and processes controlling this distribution. To this end, the study focused on major and trace elements in six rock samples (**Table 1**). This approach allows for the identification of potential genetic relationships between the rocks, determination of the magmatic source(s), and reconstruction of the geodynamic environment of emplacement using diagrams derived from major and trace element data. Specifically, the study relies on the elemental abundances, and using specialized diagrams, it evaluates the distribution of these elements among the different rock types. The chemical analyses of the rock samples collected from the study area were performed by determining major elements using X-ray fluorescence (XRF) on whole-rock powders, and trace elements using inductively coupled plasma mass spectrometry (ICP-MS). The six (6) samples selected, were reduced by cone-and-quartering to obtain a ~ 50 g subsam ple, which was then pulverized in an agate-lined puck-and ring vibratory mill to < 50 μm. Final powders were sent for whole rock analysis to Bureau Veritas in Vancouver (Can ada), where forty-eight elements were analyzed (LF600 (LF100-EXT + XF700 + TC000) package) including. A detailed description of this analytical technique is provided in [28].

4. Results

4.1. Petrographic Data

In this study, the collected rocks can be grouped into two main lithological sets: granitoids sensu stricto and migmatites (migmatized granitoids or anatexites).

4.1.1. Granitoids Sensu Stricto

Pink Granite (SEG03)

The pink granites observed in the study area were located along the Dyakala-Békoro axis (**Figure 2(A)**). They are massive and generally coarse-grained. At outcrop scale, they consist of quartz, feldspars, and biotite. Under the microscope (**Figure 2(B)**), the rock displays a porphyroblastic coarse-grained texture and is composed of the following major minerals: quartz, the most abundant mineral, with medium-sized grains often showing undulatory extinction; orthoclase occurring as medium-sized crystals; microcline, less abundant than orthoclase, generally large-grained; plagioclase, less abundant, strongly altered to sericite; and biotite, a minor mineral, brownish to greenish in color, medium-sized, and undergoing chloritization.

Biotite Granite (SEG05)

This rock was observed along the Békoro-Séguéla and Séguéla-Samadougou axes. It exhibits a coarse-grained texture. At outcrop, it is composed of quartz, plagioclase, and biotite. Microscopically (**Figure 2(C)**), the rock consists of: abundant quartz of variable grain size with pronounced undulatory extinction; highly sericitized plagioclase; less abundant microcline, occasionally containing altered plagioclase crystals; and biotite of variable size, automorphic, with myrmekitic textures characterized by fine quartz vermicules within alkali feldspar crystals.

Granodiorite (SEG07)

Observed along the Somadougou-Mamouroula axis (**Figure 2(D)**), the granodiorite is massive, mesocratic, and coarse-grained. At outcrop, it consists of quartz, plagioclase, amphibole, and biotite. Microscopically (**Figure 2(E)** and **Figure 2(F)**), the rock comprises: abundant microcline with large- to medium-sized crystals; medium-grained quartz; automorphic brown biotite; and minor pyroxene, automorphic, showing myrmekitic textures.

4.1.2. Migmatites

Biotite Migmatite (SEG08)

Observed along the Suala-Kavéna axis (**Figure 2(G)**), this rock has a coarse-grained texture and consists of quartz, feldspars, and biotite at the outcrop scale. Microscopically, it shows a porphyroblastic coarse-grained texture and is composed of: quartz, the most abundant, anhedral, with undulatory extinction; microcline, also abundant, generally large, sometimes strongly altered to sericite, with grid-like twinning; biotite, automorphic, brownish to greenish, variable in size; and minor myrmekite, consisting of fine vermicules of quartz and plagioclase, which is less abundant and anhedral to subhedral.

Biotite-Amphibole Migmatite (SEG02)

Observed along the Békoro-Séguéla axis, this rock shows an outcrop foliation of N50˚ - 60˚ NW and a left-lateral shear along N110˚. It exhibits a coarse-grained texture and is composed mainly of quartz, feldspars, and biotite. Microscopically (**Figure 2(I)**), it contains: abundant anhedral quartz with undulatory extinction; microcline, less abundant than quartz, generally large, with grid-like twinning; minor subhedral amphibole with two basal cleavages intersecting at ~120˚; biotite, often included in amphiboles, greenish in color; minor pyroxene, anhedral to subhedral; and garnet, automorphic, less abundant, included in pyroxene.

Biotite-Amphibole-Pyroxene Migmatite (SEG09)

Located along the Kavéna-Séguéla and Séguéla-Nyanangoro axes, this rock shows a left-lateral shear at N30˚ at outcrop. It has a porphyroblastic coarse-grained texture and consists of quartz, feldspars, and biotite. Microscopically (**Figure 2(H)**), it comprises: abundant anhedral quartz with pronounced undulatory extinction; less abundant large-grained microcline with grid-like twinning; biotite as automorphic to subautomorphic phenocrysts, brown to greenish; minor myrmekite, occurring as fins quartz vermicules; minor pyroxene, anhedral to subhedral; and titanite, pale yellow in color.

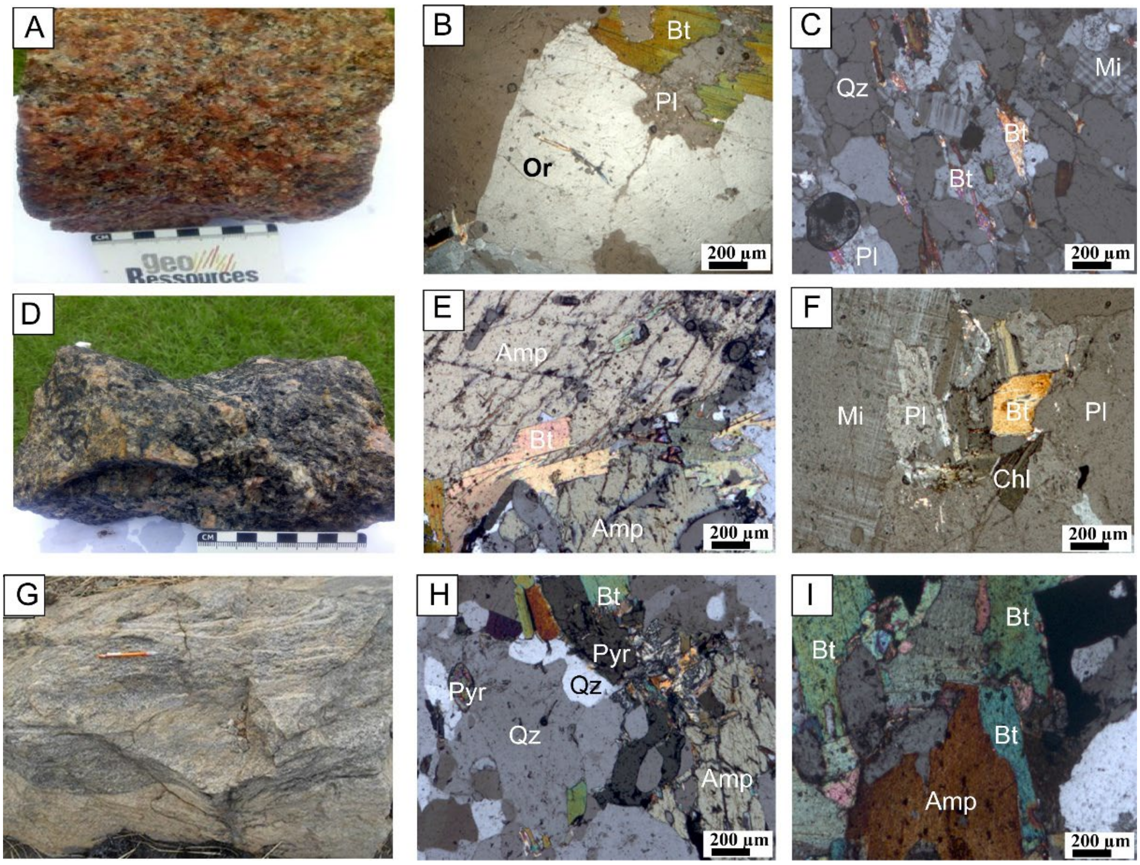

Figure 2. Macroscopic and microscopic features of granitoids and migmatites from the study area. A and B—Macrophotograph and microphotograph of pink granite (SEG03), respectively. C—Microphotograph of biotite granite. D—Photograph of granodiorite (SEG07). E-F—Microphotographs of granodiorite (SEG07). G—Photograph of biotite migmatite. H—Microphotograph of biotite-amphibole-pyroxene migmatite. I—Microphotograph of biotite-amphibole migmatite. Mineral abbreviations: Bt: biotite; Or: orthoclase; Mi: microcline; Amp: amphibole; Pyr: pyroxene; Qz: quartz; Pl: Plagioclase; Chl: Chlorite.

4.2. Geochemistry of the Séguéla Granitoids

4.2.1. Major and Trace Elements

To characterize the granitoids, the chemical compositions of the collected samples were plotted on various rock classification diagrams. In the normative Q'/ANOR diagram of [29] (**Figure 3(A)**), the Séguéla granitoids show trends from monzogranitic (SEG2, SEG3, SEG5, and SEG8) to granodioritic compositions (SEG7 and SEG9).

Granites

These rocks are characterized by high contents of SiO_2 (70.6% - 73.1%), Al_2O_3

(13.9% - 14.8%), and K_2O (3.93% - 4.44%), and low contents of Fe_2O_3 (1.85% - 2.37%), MgO (0.43% - 0.52%), TiO_2 (0.23% - 0.24%), and CaO (1.63% - 2.21%) (**Table 1**). In the diagram of [30] (**Figure 3(B)**), these granites display a slightly peraluminous and strongly calc-alkaline character, as confirmed by the K_2O vs. SiO_2 binary diagram of [31] (**Figure 3(C)**).

Granodiorites

This rock type is characterized by SiO_2 = 65.6%, Al_2O_3 = 15.2%, MgO = 2.08%, Fe_2O_3 = 4.92%, CaO = 3.54%, and TiO_2 = 0.6%. The diagram of [30] indicates that it is metaluminous (**Figure 3(B)**) and calc-alkaline, as shown in the K_2O vs. SiO_2 diagram of [31] (**Figure 3(C)**).

Migmatites

These rocks display SiO_2 contents ranging from 64.8% to 71.2%, MgO from 0.65% to 2.4%, Fe_2O_3 from 2.32% to 6.66%, Al_2O_3 from 14.4% to 14.6%, and CaO from 1.74% to 3.64%. Na_2O and K_2O vary from 3.76% to 4.22% and 1.9% to 5.16%, respectively, while TiO_2 ranges from 0.27% to 0.65%. Migmatites are generally metaluminous to slightly peraluminous (**Figure 3(B)**). In the K_2O vs. SiO_2 diagram of [31], the migmatites plot within the shoshonitic and calc-alkaline fields (**Figure 3(C)**).

The projection of the different granitoids (granites, granodiorites, and migmatites) from the study area onto Harker-type diagrams [32] (**Figure 4**) shows a linear distribution, with a negative correlation between SiO_2 and most other oxides (Al_2O_3, Fe_2O_3, CaO, MgO, MnO, Na_2O, and TiO_2), except for K_2O, which exhibits a positive correlation.

Table 1. Major and trace element composition of granitoids and migmatites from the Séguéla region.

	Granites		Granodiorite	Migmatites		
Samples	SEG03	SEG05	SEG07	SEG08	SEG09	SEG02
wt%						
SiO_2	73.1	70.6	65.6	71.2	64.8	70.4
Al_2O_3	13.9	14.8	15.2	14.4	14.5	14.6
Fe_2O_3	1.85	2.37	4.92	2.53	6.66	2.32
CaO	1.63	2.21	3.54	1.77	3.64	1.74
MgO	0.43	0.52	2.08	0.65	2.4	0.69
Na_2O	3.59	3.9	4.39	3.84	4.22	3.76
K_2O	4.44	3.93	2.53	4.18	1.9	5.16
MnO	0.02	0.02	0.08	0.04	0.09	0.05
TiO_2	0.24	0.23	0.6	0.34	0.65	0.27
P_2O_5	0.07	0.12	0.23	0.13	0.14	0.09
LOI	0.18	−0.06	0.16	0.2	0.25	−0.04
SUM	99.45	98.64	99.33	99.28	99.25	99.04
A/CNK	1.02	1.01	0.93	1.02	0.93	0.98

Continued

Trace elements						
Ba	1433	1512	940	1168	426	1260
Co	3.3	3.3	12	4.3	18.5	4.4
Cs	0.7	0.7	1.1	2	4.3	1.3
Hf	3.9	6.7	4.5	5.7	4.8	3.1
Nb	6.1	4.3	14.7	7.6	7.3	15.4
Rb	130.6	98.8	82.1	158.7	132.4	187.3
Sn	<1	<1	3	1	1	2
Sr	462.9	569.1	546.2	428.4	416.1	406.5
Ta	0.2	0.4	1	0.3	0.7	1.8
Th	5.2	14	8.9	15.8	6.4	9.7
U	0.9	0.9	0.6	1.3	7.4	1.9
Zr	141.5	255.9	172.7	212.8	189.1	118.3
Y	3.6	5.5	31.4	9.7	16	21.6
Rare earth elements (REE)						
La	29.5	43.1	57.7	60.5	34.4	33.9
Ce	54	82.3	97.2	119.5	66.6	68.6
Pr	5.28	7.9	12.04	11.96	7.51	7.82
Nd	16.7	25.4	46	41.3	28.4	29.8
Sm	1.86	3.24	8.65	5.72	4.84	6
Eu	1.03	0.92	1.65	1.23	1.21	1.02
Gd	1.3	2.13	7.31	3.49	4.05	5.18
Tb	0.15	0.28	1.12	0.38	0.56	0.81
Dy	0.71	1.24	5.83	1.88	3.12	4.45
Ho	0.11	0.21	1.13	0.3	0.61	0.79
Er	0.35	0.51	3.12	0.9	1.68	2.15
Tm	0.05	0.08	0.41	0.12	0.27	0.29
Yb	0.37	0.48	2.33	0.82	1.69	1.75
Lu	0.06	0.06	0.3	0.12	0.27	0.2
R	111.47	167.85	244.79	248.22	155.21	162.76
Calculate elements ratios						
LaN/YbN	52.65	59.29	16.35	48.72	13.44	12.79
LaN/SmN	9.67	8.11	4.07	6.45	4.33	3.44
GdN/YbN	2.82	3.56	2.52	3.42	1.92	2.38
Eu/Eu*	2.046	1.082	0.641	0.85	0.844	0.565

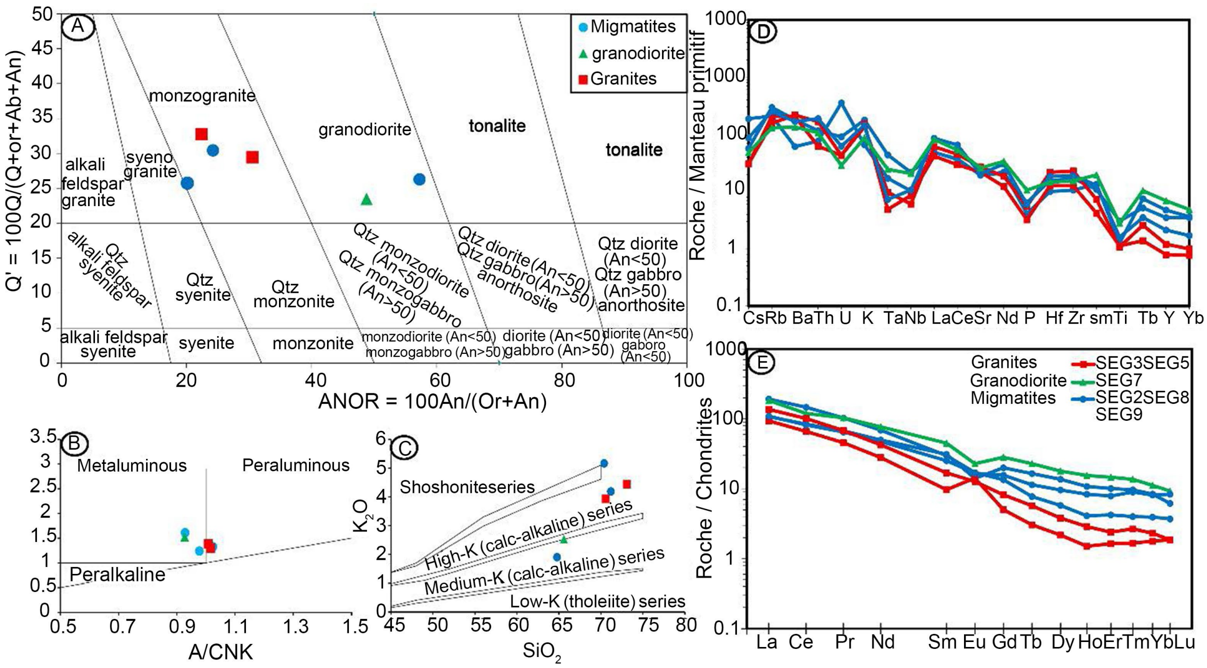

Figure 3. Positions of granitoids and migmatites in various rock classification, nomenclature, and differentiation diagrams. A—Normative Q'/ANOR diagram [29]. B—A/NK vs. A/CNK diagram [30]. C—Binary K_2O vs. SiO_2 diagram [31]. D—Primitive mantle-normalized multi-element diagram [33]. E—Chondrite-normalized REE spectra [34].

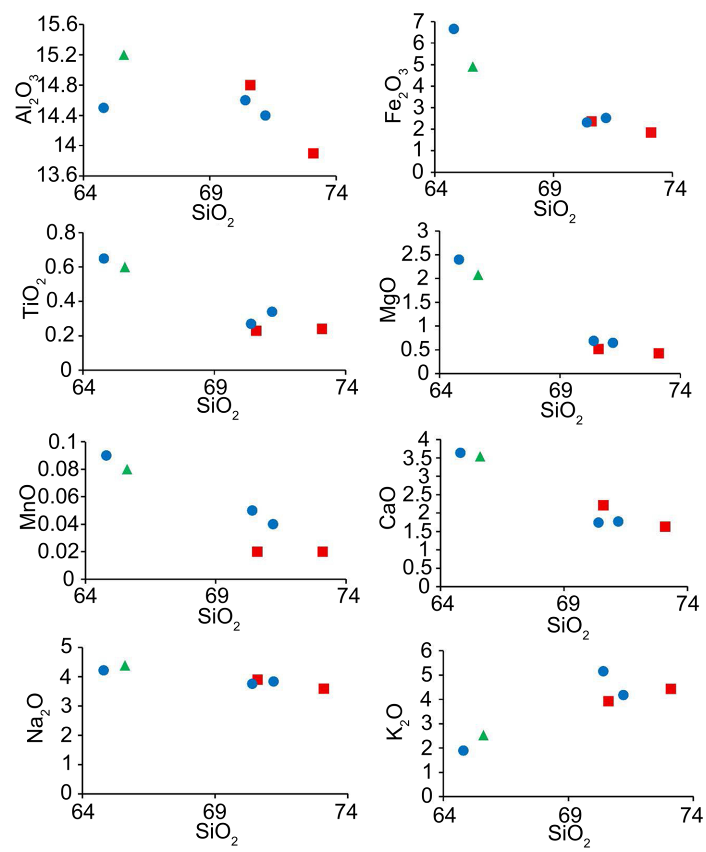

Figure 4. Granitoids and migmatites from the study area plotted on oxide vs. SiO_2 Harker-type diagrams [32]. Legend as in **Figure 3(A)**.

The granites, granodiorites, and migmatites exhibit variable trace element contents. Notably, elements such as Ba, Rb, Sr, and Zr show relatively high concentrations. Among these, the granites display the highest Ba contents (1433 - 1512 ppm) compared to the granodiorites and migmatites (**Table 1**).

In the primitive mantle-normalized multi-element diagram of [33] (**Figure 3(D)**), the spectra overall show enrichment in Rb and K, and to a lesser extent in Ba, for both granites and granodiorites. A depletion in Nb, Ta, Sr, Cs, P, and Ti is observed in all rock types. Additionally, a moderate to slight enrichment in Hf and Zr is noted. All rocks display a negative U anomaly, except for the migmatite SEG9, which exhibits a pronounced enrichment.

4.2.2. Rare Earth Elements (REE)

The total REE (ΣREE) contents of the granites are generally high, ranging from 111.47 to 167.85 ppm. The granites show negative slopes, reflecting a fractionation ratio $(La/Yb)_N$ of 52.65 - 59.29. When normalized to chondrites [34], the spectra indicate LREE enrichment with $(La/Sm)_N$ ratios of 8.11 - 9.66, and HREE depletion with $(Gd/Yb)_N$ ratios of 2.52 - 3.56. These rocks also exhibit positive Eu anomalies, except for sample SEG03 (**Figure 3(E)**), with *Eu*/*Eu ratios** of 1.08 - 2.04.

The granodiorite has a high ΣREE (244.79 ppm) and shows a negative slope with a $(La/Yb)_N$ of 16.35, indicating significant LREE enrichment ($(La/Sm)_N$ = 4.07) and HREE depletion. It exhibits a pronounced negative Eu anomaly (Eu/Eu* = 0.64) (**Figure 3(E)**).

The migmatites have ΣREE values ranging from 155.21 to 248.22 ppm, with negative slopes and $(La/Yb)_N$ ratios between 12.79 and 48.71, reflecting LREE enrichment ($(La/Sm)_N$ = 3.44 – 6.44) and HREE depletion ($(Gd/Yb)_N$ = 1.92 – 3.41). They also display strong negative Eu anomalies (Eu/Eu* = 0.56 – 0.85) and a slight tendency toward negative Ce anomalies (Ce/Ce* = 0.97 – 1.04) (**Figure 3(E)**).

5. Discussion

The study area is located in the central part of the Archean-Proterozoic transition zone defined by [4] [26], where Archean relics have been identified within the juvenile Birimian formations. The kimberlitic dykes of the Séguéla region crosscut two granite plutons separated by small amphibolite panels belonging to the Paleoproterozoic Birimian formations of the West African Craton. These are biotite- and hornblende-bearing monzonitic granites, exhibiting differentiated pegmatitic and aplitic cupolas as well as porphyroid margins [1]. They have been Pb/Pb dated at 3132 ± 9 Ma to 3141 ± 2 Ma [4]. The kimberlitic structures do not crop out naturally, as they are covered by several meters of colluvium. The granitoids belong to the granito-gneissic complexes of the Séguéla region. Our study confirms the presence of granites, granodiorites, and migmatites. Petrographically, these rocks are dominated by quartz and feldspars, with microcline more abundant than plagioclase, which is often sericitized and occurs as myrmekite. This mineral is considered metasomatic, associated with tectonic activity [35].

Metasomatism has been suggested [11] as responsible for microclination of feldspars in Eburnean granitoids, resulting in increased potassium content. This phenomenon is also observed in Archean formations and can be attributed to varying degrees of crustal recycling within the West African Craton during the Eburnean [17] [25] [36]-[38]. The migmatitic nature of the studied granitoids suggests a crustal anatectic origin, supported by field observations of magmatic banding, reflecting segregation between granite neosome and granodiorite paleosome [39].

Geochemically, the Séguéla granitoids exhibit a metaluminous to slightly peraluminous character and a calc-alkaline to shoshonitic trend, marked by K_2O enrichment. This potassium enrichment is accompanied by an increase in SiO_2, as shown in the Harker diagrams [32] (**Figure 4**). According to [40], peraluminous characteristics indicate a crustal affinity, whereas metaluminous signatures suggest a mantle contribution, implying a dual origin for the Séguéla granitoids. This aligns with previous studies [13] [41] reporting dual origins for Ivorian granitoids. According to [42] [43], A/CNK ratios between 1 and 1.1 correspond to granitoid generations of I- and S-type, indicating a possible mixture of metaluminous magmas with more differentiated crustal assimilation. The opposite trends observed in the Harker binary diagrams of Al_2O_3/SiO_2 and K_2O/SiO_2, as well as the negative Sr and Eu anomalies and positive Eu anomalies in the granites, reflect the mixing of two chemically distinct sources or magmatic assimilation. The similar patterns of multi-element and rare earth element (REE) spectra for the granitoids and migmatites may suggest a common origin for the formation of these rocks.

The potassic nature of these granitoids can also be explained by rock evolution: more differentiated rocks tend to be richer in potassium [10]. However, potassium and biotite enrichment may also reflect crustal metasomatism. For instance, [44] studying Ouahigouya granitoids (Burkina Faso) attributes high potassium to the progressive breakdown of ferromagnesian minerals, particularly biotite, which releases potassium into the evolving rock.

The similarities in REE and multi-element patterns among granites, granodiorites, and migmatites suggest a common magmatic source. Positive Eu anomalies in granites versus negative anomalies in granodiorites and migmatites indicate that granites likely formed by partial melting of a moderately differentiated crustal protolith, and enriched in residual plagioclase. Overall, the granitoids and migmatites were likely generated in subduction-related zones, akin to Archean TTGs [45]. Subduction-induced fluid release facilitated the formation of K-rich pink granites.

6. Conclusions

This study provides a petrographic and geochemical characterization of the Séguéla granitoids.

Petrographically, the rocks are predominantly quartz-feldspar, with main ferromagnesians being green-brown biotite and green hornblende. The dominance of microcline likely reflects metasomatism linked to Eburnean tectonics, affecting much of the West African Craton.

Geochemically, the analyzed rocks define a calc-alkaline to slightly shoshonitic chemistry for migmatites. Both granitoids and migmatites are metaluminous to peraluminous, with strong LILE enrichment (Cs, Ba, Rb, K) and pronounced Nb-Ta depletion, indicating a subduction-related environment (or remelting of a subduction-derived source). The REE patterns are consistent with this geodynamic setting, resembling Archean TTGs, suggesting formation through subduction-related melting of mafic and ultramafic rocks transformed into eclogite, followed by crustal recycling. Indeed, these rocks exhibit high $(La/Yb)_N$ fractionation rates ranging from 12.79 to 59.29 and heavy rare earth element (HREE) depletion with $(Gd/Yb)_N$ ratios ranging from 1.92 to 3.56.

Future work should include geochronological studies (trace elements and isotopes) to determine the ages of these granitoids and migmatites, identify their protoliths, and perform structural analyses to evaluate the tectonic relationships within the study area and better define their Archean character.

Acknowledgements

I would like to express my sincere gratitude to PASRES (Strategic Support Program for Scientific Research) and to the T2GEM project (Geophysical and Geochemical Technologies for Mining Exploration) for funding this research.

Conflicts of Interest

The authors declare no conflicts of interest regarding the publication of this paper.

References

[1] Allialy, M.E. (2006) Pétrologie et géochimie des kimberlites diamantifères de Séguéla (Centre-Ouest de la Côte d'Ivoire). Thèse de Doctorat, Université De Cocody Abidjan Site Officiel.

[2] Camil, J. (1984) Pétrographie, chronologie des ensembles granulitiques archéens et formations associées de la région de Man (Côte d'Ivoire): Implication pour l'histoire géologique du craton Ouest-Africain. Thèse, Université Félix Houphouët-Boigny.

[3] Boher, M. (1991) Croissance crustale en Afrique de l'Ouest à 2.1 Ga. Apport de la géochimie isotopique. Université de Lorraine.

[4] Kouamelan, A.N. (1996) Géochronologie et géochimie des formations archéennes et protérozoïques de la dorsale de Man en Côte d'Ivoire implications pour la transition Archéen Protérozoïque. Geosciences Rennes.

[5] Djro, S. (1998) Evolutions tectono-métamorphiques des gneiss granulitiques archéens du secteur de Biankouma-Touba (Nord-Ouest de la Côte-d'Ivoire). Thèse d'Etat, The University of Abidjan.

[6] Bessoles, B. (1977) Géologie de l'Afrique. Le craton Ouest-Africain. *French Geological Survey*, **88**, 402.

[7] Yacé, I. (2002) Initiation à la géologie. L'exemple de la côte d'ivoire et de l'Afrique de l'ouest. Pétrologie et Géologie régional. Edition CEDA.

[8] Pothin, K.B.K. (1988) Pétrographie et géochimie des formations précambriennes de la région d'Odienné (Nord-Ouest de la Côte d'Ivoire). Typologie du volcanisme birimien. Tendances évolutives du magmatisme éburnéen. Géochimie de l'Uranium et du Thorium dans les granitoïdes. Thèse, Université Félix Houphouët-Boigny.

[9] Bodin, L. (1951) Contribution à l'étude des granites birrimiens dans le Précambrien de l'Afrique occidentale. *Bulletin de la Direction des Mines de l'A.O.F*, **12**, 113p.

[10] Tagini, B. (1971) Esquisse structurale de la Côte d'Ivoire. Thèse de l'Université de Lausanne et publication SODEMI.

[11] Casanova, R. (1973) Géochimie et minéralogie des granitoïdes Côte d'Ivoire. Thèse de Doctarat d'Etat és-Science, Université Côte d'Azur.

[12] Yobou, R. (1993) Pétrologie des granitoïdes du protérozoïque inférieur du centre-nord de la Côte d'Ivoire (Ferkéssédougou-Marabadiassa). Evolution magmatique et contexte géodynamique. Thèse de Doctorat, Université de Paris-sud centre d'Orday.

[13] Doumbia, S. (1997) Géochimie, géochronologie et géologie structurale des formations birimiennes de Katiola-Marabadiassa (Centre-Nord de la Côte d'Ivoire): Evolution magmatique et contexte géodynamique du paléoprotérozoïque. Thèse de Doctorat, Université d'Orléans.

[14] Ouattara, G. (1998) Structure du batholite de Ferkessédougou (secteur de Zuénoula, Côte d'Ivoire). Implication sur l'interprétation de la géodynamique du paléoprotérozoïque de l'Afrique de l'ouest à 2,1 Ga. Thèse, Université d'Orléans.

[15] Camil, J. (1981) Un exemple de métamorphisme prograde de la base du faciès des amphibolites au faciès des granulites dans la region de Man (Ouest de la Côte d'Ivoire). *Comptes rendus de l'Académie des Sciences*, **293**, 513-518.

[16] Thiéblemont, D. (2001) A 3.5 Ga Granite-Gneiss Basement in Guinea: Further Evidence for Early Archean Accretion within the West African Craton. *Precambrian Research*, **108**, 179-194. https://doi.org/10.1016/s0301-9268(00)00160-1

[17] Thiéblemont, D., Goujou, J.C., Egal, E., Cocherie, A., Delor, C., Lafon, J.M., *et al.* (2004) Archean Evolution of the Leo Rise and Its Eburnean Reworking. *Journal of African Earth Sciences*, **39**, 97-104. https://doi.org/10.1016/j.jafrearsci.2004.07.059

[18] Caen-Vachette, M., Tempier, P. and Camil, J. (1984) Age Rb/Sr de 1670 M.a. pour les mylonites de l'accident du Sassandra (Côte d'Ivoire) conséquence pour la datation des mouvements fini-éburnéens dans le craton ouest-africain. *Journal of African Earth Sciences*, **2**, 359-363. https://doi.org/10.1016/0899-5362(84)90009-5

[19] Cahen, L., Snelling, N.J., Delhal, J. and Vail, J.R. (1984) The Geochronology and Evolution of Africa. Carendon Press.

[20] Liégeois, J.P., Claessens, W., Camara, D. and Klerkx, J. (1991) Short-Lived Eburnian Orogeny in Southern Mali. Geology, Tectonics, U-Pb and Rb-Sr Geochronology. *Precambrian Research*, **50**, 111-136. https://doi.org/10.1016/0301-9268(91)90050-k

[21] Gouedji, F., Picard, C., Coulibaly, Y., Audet, M., Auge, T., Goncalves, P., *et al.* (2014) The Samapleu Mafic-Ultramafic Intrusion and Its Ni-Cu-Pge Mineralization: An Eburnean (2.09 Ga) Feeder Dyke to the Yacouba Layered Complex (man Archean Craton, Western Ivory Coast). *Bulletin de la Société Géologique de France*, **185**, 393-411. https://doi.org/10.2113/gssgfbull.185.6.393

[22] Kouamelan, A.N., Kra, K.S.A., Djro, S.C., Paquette, J. and Peucat, J. (2018) The Logoualé Band: A Large Archean Crustal Block in the Kenema-Man Domain (man-Leo Rise, West African Craton) Remobilized during Eburnean Orogeny (2.05 Ga). *Journal of African Earth Sciences*, **148**, 6-13. https://doi.org/10.1016/j.jafrearsci.2017.09.004

[23] Feybesse, J.L., Milesi, J.P., Johan, V., Doget, A., Calvez, J.Y., Boher, M. and Abouchami, W. (1989) La limite archéen/protérozoïque inférieur de l'Afrique de l'Ouest: Une forme de chevauchement majeure antérieure à l'accident de Sassandra; l'exemple de la région d'Odienné et de Touba (Côte d'Ivoire). *Geochimica et Cosmochimica Acta*, **65**, 1499-1527.

[24] Pitra, P., Kouamelan, A.N., Ballèvre, M. and Peucat, J. (2010) Palaeoproterozoic High-Pressure Granulite Overprint of the Archean Continental Crust: Evidence for Homogeneous Crustal Thickening (Man Rise, Ivory Coast). *Journal of Metamorphic Geology*, **28**, 41-58. https://doi.org/10.1111/j.1525-1314.2009.00852.x

[25] Kouamélan, A.N., Peucat, J.J. and Delor, C. (1997) Reliques archéennes (3.15 Ga) au sein du magmatisme birrimien (2.1 Ga) de Côte-d'Ivoire, craton-ouest africain. *Comptes rendus de l'Académie des Sciences*, **324**, 719-727.

[26] Kouamelan, A.N., Djro, S.C., Allialy, M.E., Paquette, J. and Peucat, J. (2015) The Oldest Rock of Ivory Coast. *Journal of African Earth Sciences*, **103**, 65-70. https://doi.org/10.1016/j.jafrearsci.2014.12.004

[27] Bagarre, E. and Tagini, B. (1965) Carte géologique de la Côte d'Ivoire au 1/1 000 000. Directorate of Mines & Geology, Abidjan.

[28] Brou, J.K., Van Lichtervelde, M., Kouamelan, N.A., Baratoux, D. and Thébaud, N. (2022) Petrogenetic Relationships between Peraluminous Granites and Li-Cs-Ta Rich Pegmatites in South Issia Zone (Central-West of Côte d'Ivoire): Petrography, Mineralogy, Geochemistry and Zircon U-Pb Geochronology. *Mineralogy and Petrology*, **116**, 443-471. https://doi.org/10.1007/s00710-022-00790-2

[29] Streckeisen, A. and Le Maitre, R.W. (1979) A Chemical Approximation to the Modal QAPF Classification of the Igneous Rocks. *Neues Jahrbuch für Mineralogie*, *Abhandlungen*, **136**, 169-206.

[30] Shand, S.J. (1922) The Problem of the Alkaline Rocks. *Proceedings of the Geological Society of South Africa*, **25**, 19-33.

[31] Rickwood, T. (1989) Boundary Lines within Petrologic Diagrams Which Use Oxides of Major and Minor Elements. *Lithos*, **22**, 247-263. https://doi.org/10.1016/0024-4937(89)90028-5

[32] Harker, A. (1909) The Natural History of Igneous Rocks. Macmillan.

[33] Sun, S.S. and McDonough, W.F. (1989) Chemical and Isotopic Systematics of Oceanic Basalts: Implications for Mantle Composition and Processes. *Geological Society*, *London*, *Special Publications*, **42**, 313-345. https://doi.org/10.1144/gsl.sp.1989.042.01.19

[34] McDonough, W.F. and Sun, S. (1995) The Composition of the Earth. *Chemical Geology*, **120**, 223-253. https://doi.org/10.1016/0009-2541(94)00140-4

[35] Garcia, D., Pascal, M. and Roux, J. (1996) Hydrothermal Replacement of Feldspars in Igneous Enclaves of the Velay Granite and the Genesis of Myrmekites. *European Journal of Mineralogy*, **8**, 703-718. https://doi.org/10.1127/ejm/8/4/0703

[36] Block, S., Ganne, J., Baratoux, L., Zeh, A., Parra-Avila, L.A., Jessell, M., *et al*. (2015) Petrological and Geochronological Constraints on Lower Crust Exhumation during Paleoproterozoic (Eburnean) Orogeny, NW Ghana, West African Craton. *Journal of Metamorphic Geology*, **33**, 463-494. https://doi.org/10.1111/jmg.12129

[37] Koffi, Y.A. (2019) Evolution tectono-métamorphique du craton ouest-africain: Exemple du secteur grand-Béréby à Sassandra (SW de la Côte d'Ivoire). Thèse de l'Université FHB d'Abidjan-Cocody.

[38] Koffi, G.R., Kouamelan, A.N., Allialy, M.E., Coulibaly, Y. and Peucat, J. (2020) Re-

evaluation of Leonian and Liberian Events in the Geodynamical Evolution of the Man-Leo Shield (West African Craton). *Precambrian Research*, **338**, Article 105582. https://doi.org/10.1016/j.precamres.2019.105582

[39] Dago, A.G.B., Coulibaly, Y. and Ouattara, Z. (2019) Typologie pétrographique et géochimique des granitoïdes de la région de Daloa au Centre Ouest de la Côte d'Ivoire. *Afrique Science*, **15**, 208-221.

[40] Debon, F., Le Fort, P. and Sonet, J. (1983) Chemical-Mineralogical Typology, Chronology and Geodynamic Setting of the Western Hindu Kush–Badakhshan Plutonic Belt (Afghanistan). In: Shams, F.A., Ed., *Granites of Himalayas*, *Karakorum and Hindu Kush*, Institute of Geology, 407-423.

[41] Bard (1974) Evolution géotectonique de craton ouest-africain en Côte d'Ivoire: Elément d'un nouveau schéma. *Comptes rendus de l'Académie des Sciences*, **278**, 2039-2056.

[42] Chappell, B.W. and White, A.J.R. (1992) I and S-Type Granites in the Lachlan Fold Belt. In: *Geological Society of America Special Papers*, Geological Society of America, 1-26. https://doi.org/10.1130/spe272-p1

[43] Chappell, B.W. and White, A.J.R. (1974) Two Contrasting Granite Types. *Pacific Geology*, **8**, 173-174.

[44] Gamsonre, P.E. (1975) Contribution à l'étude géologique des formations précambriennes de la région de Ouahigouya (Burkina Faso). Université de Besançon.

[45] Martin, H., Moyen, J., Guitreau, M., Blichert-Toft, J. and Le Pennec, J. (2014) Why Archaean TTG Cannot Be Generated by MORB Melting in Subduction Zones. *Lithos*, **198**, 1-13. https://doi.org/10.1016/j.lithos.2014.02.017